SCIENCE CHINA
Technological Sciences

•Article•

https://doi.org/10.1007/s11431-023-2603-2

A double-layer radiative cooling coating that utilizes the refractive index difference between layers to achieve extremely high solar reflectivity

WANG FuQiang[1], LI ChunZhe[1,2], YANG ZhenNing[1,2], XIE WeiXin[2], LI Xiang[3], XU ZengHui[3], YAN YuYing[4] & CHENG ZiMing[2,3*]

[1] *School of Energy Science and Engineering, Harbin Institute of Technology, Harbin 150001, China;*
[2] *School of New Energy, Harbin Institute of Technology at Weihai, Weihai 264209, China;*
[3] *China Construction Eco-Environmental Protection Technology Co., Ltd., Suzhou 215123, China;*
[4] *Faculty of Engineering, University of Nottingham, Nottingham NG7 2RD, UK*

Received October 7, 2023; accepted January 19, 2024; published online September 10, 2024

Passive daytime radiative cooling (PDRC) technology has great potential in reducing cooling energy consumption. In order to further improve the spectral performance of PDRC coatings, current researchers mostly focus on the selection and size design of functional particles, while ignoring the optical properties enhancement effect caused by the interlayer binder. In this study, based on the principle that the refractive index difference between layers enhanced the backscattering performance of the solar spectrum, we proposed and manufactured a double-layer PDRC coating with polyvinylidene difluoride (PVDF) as the film-forming material in the upper layer and polydimethylsiloxane (PDMS) as the film-forming material in the lower layer, both filled with Al_2O_3 and SiO_2 particles. The double-layer PDRC coating exhibited excellent spectral performance that a high solar reflectivity of 98% and an emissivity of 0.95 at the "atmospheric window" band. In comparison, the solar spectrum reflectivity of the single-layer PDRC coatings based on PVDF and PDMS of the same thickness was 95% and 94.7%, respectively. Outdoor tests showed that the PDRC coating achieved a temperature decrease of up to 7.1°C under direct sunlight at noon time. In addition, the PDRC coating had excellent weather resistance, water resistance, and other basic properties. This article opens up a new idea and provides methodological guidance for the design of double-layer PDRC coatings.

double-layer radiative cooling coating, spectral modulation, interlayer refractive index, solar energy, radiative transfer

Citation: Wang F Q, Li C Z, Yang Z N, et al. A double-layer radiative cooling coating that utilizes the refractive index difference between layers to achieve extremely high solar reflectivity. Sci China Tech Sci, 2024, 67, https://doi.org/10.1007/s11431-023-2603-2

1 Introduction

In the context of global warming, building cooling systems consumed 15% of global energy production, and the resulting energy crisis also deserves attention [1–6]. Passive daytime radiative cooling (PDRC) technology, as a novel environmentally friendly cooling method, can achieve a sub-ambient temperature cooling effect without consuming any energy [7,8]. The fundamental principle of the PDRC technology for achieving cooling is to strongly reflect solar irradiance (0.3–2.5 μm) and radiate electromagnetic waves to outer space through the "atmospheric window" (ATSW, 8.0–13.0 μm) [9–12]. In the future, PDRC materials can be widely used in green buildings [13,14], facility agriculture [15], efficient solar cells [16–18], and other related fields [19–25].

The cooling effect of PDRC materials is primarily dependent on the solar spectrum reflectivity and the emissivity

*Corresponding author (email: chengzm@hit.edu.cn)

within the "atmospheric window" band [26]. For each 1% increase in solar spectrum reflectivity, an additional theoretical cooling power of approximately 10 W/m^2 can be obtained [27]. Enhancing the emissivity within the "atmospheric window" band also contributes positively to improving the cooling effect. Therefore, how to improve the performance of these two indicators was the focus of current researchers [17,28–31]. Many researchers achieve high spectral performance by designing surface structures or utilizing internal particles for enhanced electromagnetic response to achieve high optical properties [32–35]. The single-layer PDRC coating, employing a sole film-forming substance to envelop particles and producing a uniform single-layer film, has consistently remained a focal point in research as the most convenient radiative cooling material [31,36]. It was composed of filler particles, film-forming binders, and additives. The filler particles predominantly include TiO_2, $CaCO_3$, and $BaSO_4$ [20,37,38], exhibiting strong reflection of the solar spectrum, as well as SiO_2, SiC, Si_3N_4 [39], demonstrating high emissivity in the "atmospheric window" band. Commonly used binders encompass acrylic resin, polyvinylidene difluoride (PVDF), polydimethylsiloxane (PDMS), and polymethyl methacrylate (PMMA) [20,40–42].

To enhance the spectral performance of PDRC coatings, numerous researchers have devised various solutions [43–45]. For example, Luo et al. [46] developed a versatile scalable photonic film with excellent mechanical stability by combining the excellent scattering efficiency of the hexagonal boron nitride (h-BN) nanoplates. The Ecoflex@h-BN film exhibited sufficiently high solar reflectance (0.92) and ideal emissivity (0.97), and achieved sub-ambient cooling effect of 9.5°C during the continuous outdoor measurements. Currently, the design concepts for multi-layer PDRC coatings primarily involve particles in different layers playing distinct roles, yet most of them employ the same matrix. A double-layer PDRC coating was designed by Huang and Ruan [47]. According to the Mie theory, the top and bottom layers were acrylic resin embedded with TiO_2 and carbon black particles, respectively responsible for reflecting the solar irradiation and emitting the heat in the "atmospheric window". The TiO_2 particles with a size of 0.2 μm were optimized by Mie theory and solving the Radiative Transfer Equation to provide the best scattering ability. Similarly, Bao et al. [48] designed a double-layer PDRC coating with a reflective top layer and an emissive bottom layer. The top layer comprised densely packed rutile TiO_2 (D=0.5 μm) submicron particles, while the bottom layer embedded SiO_2 or β-SiC nanoparticles. The film-forming materials for the upper and lower layers were all acrylic resin. The double-layer PDRC coating exhibited solar reflectivity (90.7%) and atmospheric transmission window emittance (~90.11%). To achieve the high optical performance of the double-layer PDRC coatings, Dong et al. [49,50] introduced a masking layer for these coatings. The lower layer served as the reflection layer embedded with TiO_2 and SiO_2 particles, while the upper layer was a masking layer composed of Al_2O_3 and SiO_2 particles. The matrix of both upper and lower layer was acrylic resin. This PDRC coating achieved solar reflectivity (94.0%) and "atmospheric window" emittance (93.0%).

The literature survey indicated that in the design of double-layer PDRC coatings, researchers primarily concentrated on functional particle selection and sizing, overlooking the potential improvement in optical properties due to the interlayer binder. In this study, based on the principle that the differences in refractive indices between layers enhanced the backscattering performance of the solar spectrum, we proposed and manufactured a double-layer PDRC coating with PVDF as the film-forming material in the upper layer and PDMS as the film-forming material in the lower layer, both filled with Al_2O_3 and SiO_2 particles. The double-layer PDRC coating exhibited excellent spectral performance that a high solar reflectivity of 98% and an emissivity of 0.95 at the "atmospheric window" band. In contrast, single-layer PDRC coatings, based on PVDF and PDMS with equivalent thickness, exhibited solar spectrum reflectivity of 95% and 94.7%, respectively. Outdoor tests showed that the PDRC coating achieved a temperature decrease of up to 7.1°C under direct sunlight at noon time. Moreover, the PDRC coating demonstrates commendable weather resistance, water resistance, and other basic properties.

2 Theory design of the double-layer PDRC coating

Based on the principle that the differences in refractive indices between layers enhanced the backscattering performance of the solar spectrum, a double-layer radiative cooling coating structure was proposed, with PVDF as the film-forming substance in the upper layer and PDMS in the lower layer, both containing Al_2O_3 and SiO_2 particles, as shown in Figure 1(a). The film-forming substance PVDF and PDMS were chosen as film-forming materials for the upper and lower layers, respectively, due to their significant difference in refractive indices (Figure 1(b)).

In terms of functional particle selection, Al_2O_3 particles were used as reflective particles because of their wide semiconductor bandgap, which allows them to reflect a broad spectrum of solar energy. SiO_2 particles were selected as emitting material due to their relatively large extinction coefficient in the wavelength range of 8–13 μm. Besides, the natural wrinkles on the coating surface could also increase the emission of energy in the "atmospheric window" band, thereby enhancing the cooling capability of the coating [42].

The finite difference time domainmethod (FDTD) solution

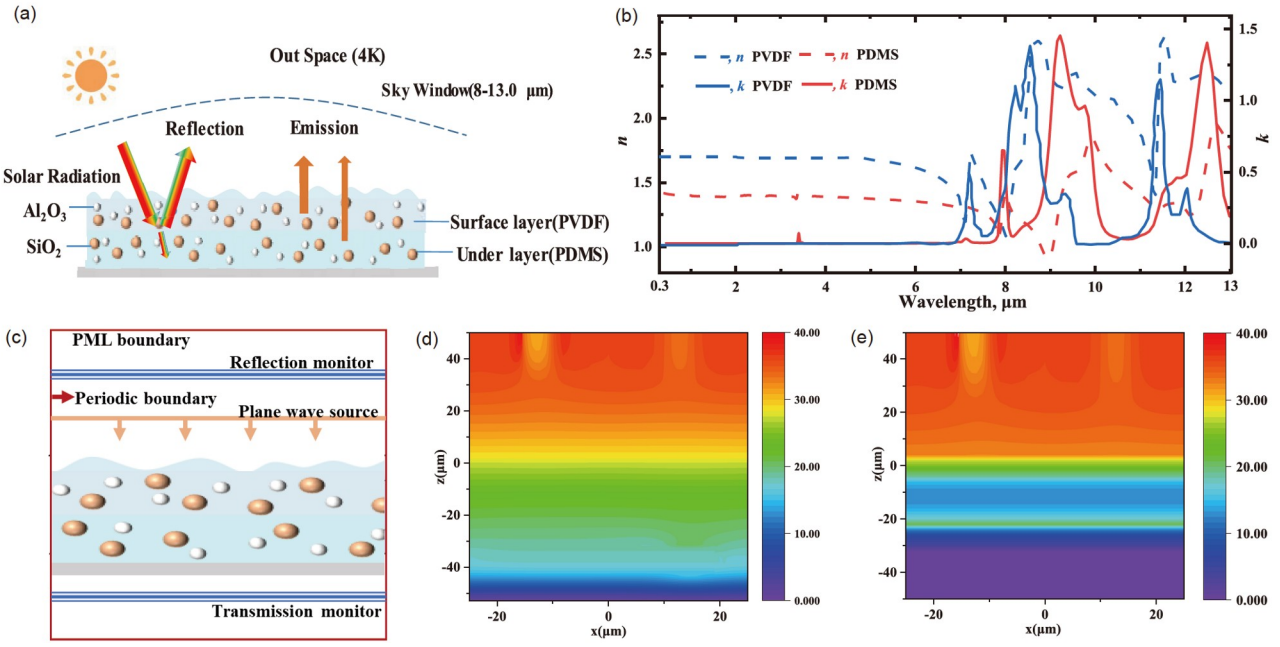

Figure 1 Theoretical verification of the double-layer design of the PDRC coating. (a) Structural diagram of the double-layer PDRC coating; (b) optical constant value of PVDF and PDMS; (c) schematic diagram of FDTD calculation parameter settings. The electromagnetic field of the double-layer PDRC coating (d) and single-layer PDRC coating (e) at incident light with a wavelength of 0.5 μm.

was used to establish a simulation model for the double-layer structure and optimize the coating parameters. The simulated incident light was set as a plane wave light source with the periodic boundary conditions (Figure 1(c)). Initially, verification of the double-layer structure's potential to enhance spectral scattering capability in the solar band was required. The electromagnetic field two-dimensional (2D) distribution in the double-layer PDRC coating (Figure 1(d)) and the single-layer coating (PVDF, Figure 1(e)) were calculated at an incident light wavelength of 0.5 μm. Comparing both figures revealed a decreasing trend in the internal wave phase of the incident light coating, while the electromagnetic field intensity of the double-layer structure coating at the interface attenuates more slowly. This illustrated that the substantial difference in refractive index between the double layers resulted in high dielectric contrast, thus augmenting the scattering capability.

Next, the particle size and volume fraction of the Al_2O_3 and SiO_2 particles were optimized. As shown in Figure 2(a) and (c), when the average diameter of the Al_2O_3 particles was 0.5 μm and the volume of the particles was 70%, the average reflectivity of the PDRC coating in the solar band reached the maximum value. SiO_2 particles with an average particle size of 4.0 μm maximize the emissivity of the PDRC coating in the wavelength range of 8.0–13.0 μm (Figure 2(b)). The further calculation of the absorption coefficient of SiO_2 in the atmospheric window band further confirms this result (Figure 2(b) inset). The reason why SiO_2 particles with the average particle size of 4 μm can effectively enhance the emissivity of the coating at 8–13 μm was that smaller particles resonate at the electric dipolar resonance while higher order electric and magnetic modes are excited in the larger particles. As shown in Figure 2(d), when the volume fraction of SiO_2 particles reaches 8%, the emissivity of the double-layer radiative cooling coating in the atmospheric window band no longer increases with an increase in volume fraction.

When the upper layer (PVDF) of the double-layer PDRC coating reached 50 μm and the overall thickness of the coating reached 100 μm, the reflectivity of the coating in the solar band basically no longer changed with the increase in thickness.

3 Preparation and characterization of the double-layer PDRC coating

As an example, for the preparation of a 200 g coating: the required raw materials included 10 g of PDMS and 32 g of *N*-methylpyrrolidone (NMP) for the bottom layer, along with 50 g of Al_2O_3 and 8 g of SiO_2 particles; for the top layer, it consisted of 12 g of PVDF and 30 g of NMP, along with 8 g SiO_2 particles and 50 g of Al_2O_3 particles.

The preparation of the double-layer PDRC coating involved a sequence of key steps encompassing particle ball-milling, precise weighing, dissolution, agitation, dual-layer application, and drying. The first step involves preparing the bottom layer of the double-layer radiative cooling coating using PDMS as the binder. Utilizing an electronic balance,

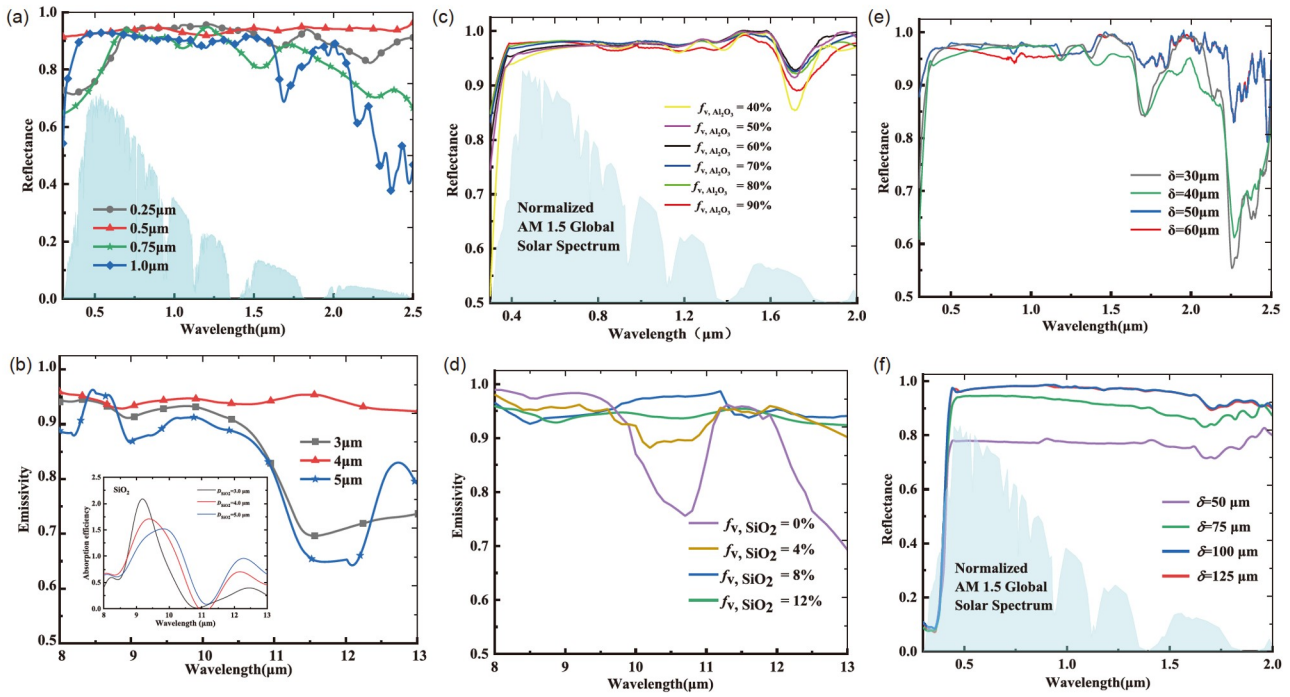

Figure 2 Optimization design of particles in the coating. Optimization design of particle size of Al_2O_3 (a) and SiO_2 (b) particles; insert was absorption efficiency of SiO_2. Optimization of volume fraction of Al_2O_3 (c) and SiO_2 (d) particles. (e) and (f) Optimization of overall coating thickness and surface layer (PVDF) thickness design.

Al_2O_3, SiO_2 particles, and PDMS binder were meticulously weighed, followed by the addition of suitable NMP to the composite. This mixture underwent ultrasonic oscillation for 15 min until achieving complete particle dispersion. Subsequently, continuous stirring at 300 r/min persisted for 8 h, ensuring comprehensive adhesive reactivity. Prior to coating, an optimal quantity of NMP (5–10 mL) was introduced to modulate the coating's viscosity until it exhibited a gradual flow down the glass rod in filamentous strands. The preparation of all test samples in this paper was conducted using a high-pressure airless spraying process. Prior to spraying, the required amount of coating was calculated, approximately 500 g/m^2. During spraying, a thin, multiple-pass spraying technique was employed, resulting in a final wet film thickness of approximately 200 μm, while the film thickness after drying was approximately 50 μm. Subsequently, the coating underwent a 10-h drying process within a controlled environment at 60°C, thereby concluding the formulation of the lower layer.

Sequentially, the upper layer (comprising PVDF) of the coating was fabricated, employing procedures akin to those aforementioned. The variance lay in the introduction of Al_2O_3, SiO_2 particles, and PVDF binder into the NMP solution to forge a composite. By subjecting it to a consistent drying temperature of 70°C for 8 h, the culmination ensued in the attainment of the double-layer PDRC coating. In pursuit of subsequent comparative analyses, the same materials and preparation methods were employed to fabricate 100 μm thickness single-layer radiative cooling coatings using PVDF and PDMS as binders, respectively.

The particle size distribution of the Al_2O_3 and SiO_2 particles was measured using a particle size analyzer. Al_2O_3 particles had a median size of 0.5 μm, with 95% of their volume fraction between 0.1 and 1.0 μm (Figure 3(b)). SiO_2 particles had a median size of 4.0 μm, and 93% of their volume fraction ranged between 1 and 8 μm, conforming to the simulation's particle size requirements (Figure 3(c)). The cross-sectional images of the double-layer radiative cooling coating were characterized using scanning electron microscopy (SEM). As shown in Figure 3(d), it was evident that the bond between the layers was very strong, while also showing the boundary line between the layers. The coating's surface morphology was examined using an optical microscope coupled with 3D analysis software, indicating wrinkle heights of approximately 5 μm, characterized as micro-nano scale wrinkles (Figure 3(e)). These wrinkles form due to differential evaporation rates during preparation and drying, resulting in surface tension; this structure positively influences both solar spectral band reflectance and atmospheric window band emissivity.

The ultraviolet-visible-near infrared (UV-VIS-NIR) spectrophotometer and Fourier transform infrared spectrometer combined with an integrating sphere were used to measure the spectral properties of PDRC coatings in the 0.3–15.0 μm bands. As shown in Figure 3(f), the double-layer PDRC coating exhibited excellent spectral performance with a high

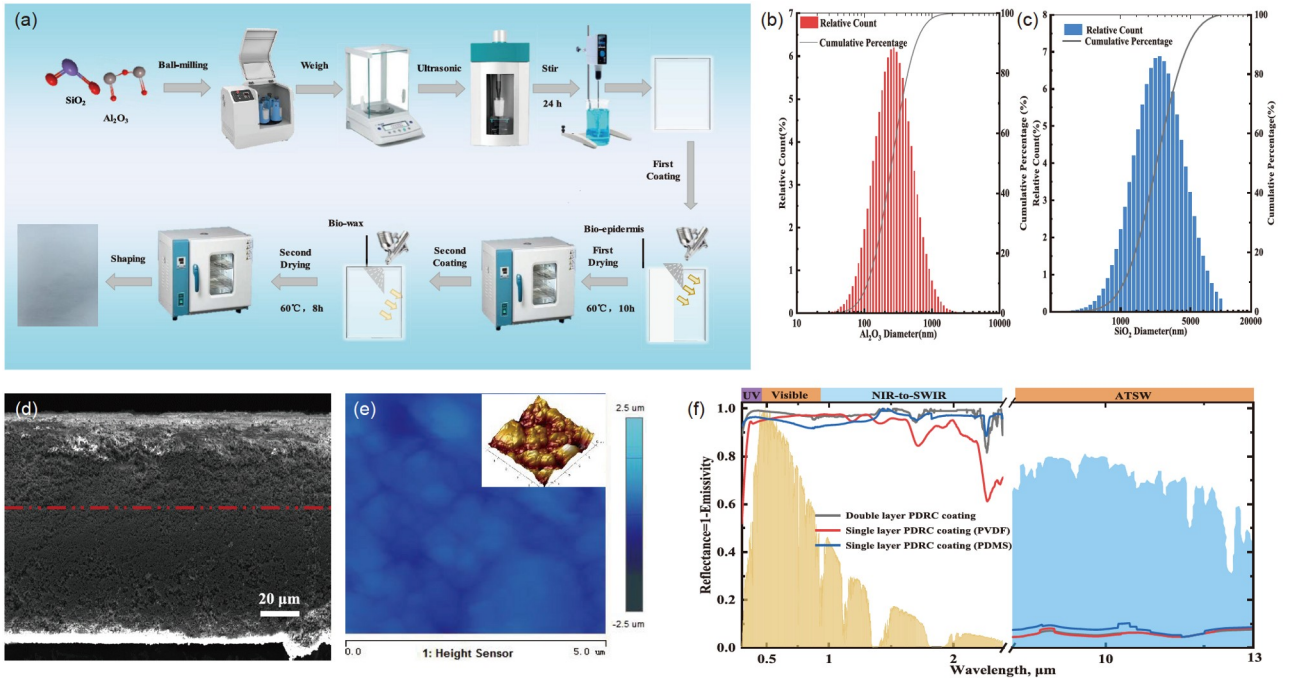

Figure 3 Testing and characterization of the double-layer PDRC coating. (a) Preparation process of the coating; (b) and (c) particle size distribution of Al_2O_3 and SiO_2 particles; (d) SEM images of the cross-section of the double-layer PDRC coating; (e) photo of the surface morphology of the coating; (f) spectral reflectivity curves of double-layer coating and single-layer coatings.

solar reflectivity of 98% and selective emission with an emissivity of 0.95 at the "atmospheric window" band. In comparison, the solar spectrum reflectivity of the single-layer PDRC coatings based on PVDF and PDMS of the same thickness was 95% and 94.7%, respectively.

4 Outdoor cooling performance test of the double-layer PDRC coating

An outdoor test experiment was conducted to evaluate the outdoor cooling performance of the double-layer PDRC coatings. The experimental setup comprised a data logger, a test chamber, and a weather station. The experiment utilized polystyrene foam with low thermal conductivity, enveloped by aluminum foil on its surface to reflect solar radiation. To mitigate convection effects, a 40 cm transparent polyethylene film surrounded the setup, leaving the top open. The double layer PDRC coatings were applied onto 10 cm×10 cm aluminum plates, with a thermocouple affixed to the plate's rear to monitor temperature changes. The four test samples included a double-layer PDRC coating, single-layer PDRC coatings (PVDF and PDMS), and color steel tiles. Real-time monitoring of solar radiation intensity, relative humidity, and wind speed was conducted using the weather station [51].

The actual outdoor radiative cooling capability of the coating was characterized on an unobstructed roof in Weihai city (37°31′46″N, 122°4′40″E, 0-m altitude) on April 1–2, 2023. As shown in Figure 4(c), continuous outdoor tests revealed that the double-layer PDRC coating achieved a cooling effect of 5–8°C lower than the ambient air temperature. Compared to other samples, the temperature of the double-layer PDRC coating consistently remained 2–3°C lower than the single-layer PDRC coatings (PVDF and PDMS) and 10–27°C lower than the color steel tile. At noon, between 10:00–14:00 on April 01, 2023, under the meteorological environmental conditions of an average solar irradiance of 736 W/m^2, an average wind speed of 1.7 m/s and an ambient humidity of 16.4%, the double-layer PDRC coating demonstrated an average sub-ambient temperature drop of 7.1°C. In contrast, the temperatures of the single-layer PDRC coating (PVDF), single-layer (PDMS) and color steel tile samples were 20°C, 2.7°C, and 3.2°C higher than the double-layer PDRC coating, respectively (Figure 4(d)). This observation highlights the superior practical cooling capacity of the double-layer PDRC coating.

5 Other performance test of the double-layer PDRC coating

The PDRC coating, a material with broad applications in construction, requires to have excellent adaptability during application and strong adherence to building surfaces. We selected three types of materials: marble, wood, and metal,

and applied coatings on the surfaces of the materials, all of which showed good adhesion (Figure 5(a)–(c)). Additionally, as an outdoor product, PDRC coatings must withstand rain erosion, necessitating superior water resistance. We conducted a 96-h water resistance test, sealing coating edges with paraffin to prevent water seepage and

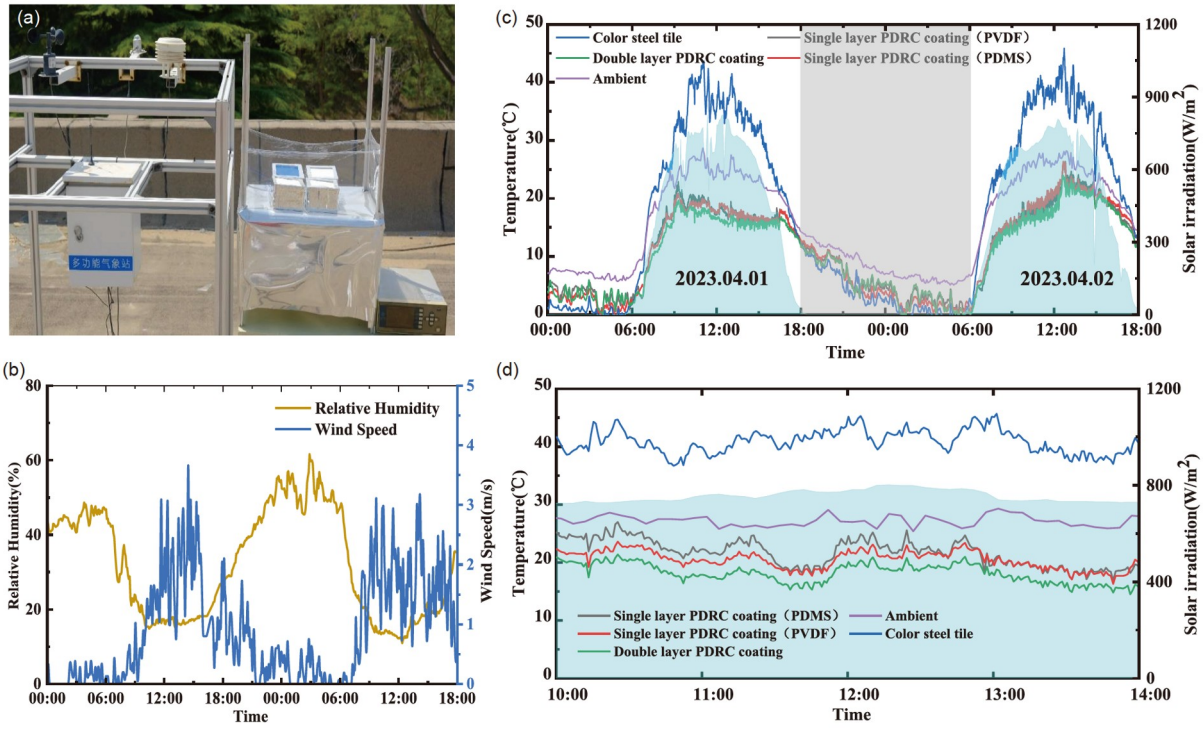

Figure 4 Outdoor test of the PDRC coating. (a) Photo of the outdoor test device; (b) relative air humidity and wind speed; (c) and (d) temperature test curves of the PDRC coating samples.

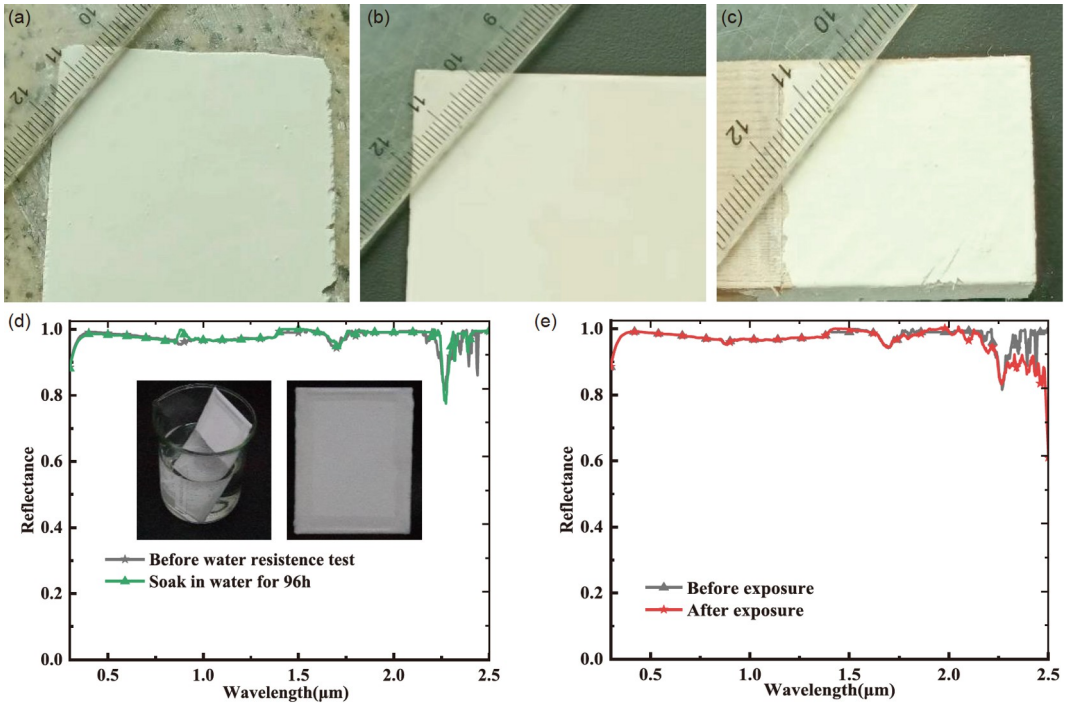

Figure 5 Other basic properties of PDRC coatings. PDRC coatings were coated on stone (a), aluminum flakes (b), and wood respectively (c); (d) spectral reflectivity of the coating before and after water resistance (insets: the test pictures); (e) comparison of spectral reflectivity of the coating before and after the exposure experiment.

corner peeling (Figure 5(d)). Post-soaking, no swelling, peeling, or discoloration occurred. The coating underwent hot air-drying, followed by testing its solar spectrum band reflectance, achieving 98% (Figure 5(d)) using a UV-VIS-NIR spectrophotometer. A 60-day outdoor durability test revealed no cracks or peeling on the coating surface. Solar spectral reflectance testing (Figure 5(e)) displayed no significant degradation in spectral performance.

6 Conclusion

In this study, based on the principle that the refractive index difference between layers enhanced the backscattering performance of the solar spectrum, we proposed and manufactured a double-layer PDRC coating with PVDF as the film-forming material in the upper layer and PDMS as the film-forming material in the lower layer, both filled with Al_2O_3 and SiO_2 particles. The double-layer PDRC coating exhibited excellent spectral performance that a high solar reflectivity of 98% and an emissivity of 0.95 at the "atmospheric window" band. In comparison, the solar spectrum reflectivity of the single-layer PDRC coatings based on PVDF and PDMS of the same thickness was 95% and 94.7%, respectively. Outdoor tests showed that the PDRC coating achieved a temperature decrease of up to 7.1°C under direct sunlight at noon time. Its temperature was 2.7°C, 3.2°C, and 20°C lower than the temperatures of single-layer PDRC coating (PVDF), single-layer coating (PDMS), and color steel tile samples. In addition, the PDRC coating has excellent weather resistance, water resistance, and other basic properties.

This work was supported by the National Natural Science Foundation of China (Grant Nos. 52306078 and 52211530089), Taishan Scholars of Shandong Province (Grant No. tsqn201812105), the Natural Science Foundation of Shandong Province (Grant No. ZR2023QE141), and the Royal Society (Grant No. IEC\NSFC\211210). A very special acknowledgment is made to the editors and anonymous peer reviewers who provided important comments that improved this paper.

1 Cheng Z M, Shuai Y, Gong D Y, et al. Optical properties and cooling performance analyses of single-layer radiative cooling coating with mixture of TiO_2 particles and SiO_2 particles. Sci China Tech Sci, 2021, 64: 1017–1029
2 Zhou N, Li Y. PtFe and Fe_3C nanoparticles encapsulated in Fe–N-doped carbon bowl toward the oxygen reduction reaction. Int J Hydrogen Energy, 2023, 48: 13591–13602
3 Liu M, Li X, Li L, et al. Continuous photothermal and radiative cooling energy harvesting by VO_2 smart coatings with switchable broadband infrared emission. ACS Nano, 2023, 17: 9501–9509
4 Zhai H, Fan D, Li Q. Dynamic radiation regulations for thermal comfort. Nano Energy, 2022, 100: 107435
5 Zhang P, Qiu Y, Ye C, et al. Anisotropically conductive phase change composites enabled by aligned continuous carbon fibers for full-spectrum solar thermal energy harvesting. Chem Eng J, 2023, 461: 141940
6 Luo D, Yan Y, Chen W H, et al. A comprehensive hybrid transient CFD-thermal resistance model for automobile thermoelectric generators. Int J Heat Mass Transfer, 2023, 211: 124203
7 Chen M, Pang D, Yan H. Colored passive daytime radiative cooling coatings based on dielectric and plasmonic spheres. Appl Thermal Eng, 2022, 216: 119125
8 Hu D, Gu Y. A membrane reflector, polymer hybrid infrared emitter for better radiative cooling performance. Sol Energy Mater Sol Cells, 2022, 234: 111417
9 Chen M, Pang D, Chen X, et al. Passive daytime radiative cooling: Fundamentals, material designs, and applications. EcoMat, 2021, 4: 12153
10 Wang C H, Chen H, Jiang Z Y, et al. Design and experimental validation of an all-day passive thermoelectric system *via* radiative cooling and greenhouse effects. Energy, 2023, 263: 125735
11 Hu M, Zhao B, Suhendri B, et al. Effect of vacuum scheme on radiative sky cooling performance. Appl Thermal Eng, 2023, 219: 119657
12 Zhao B, Xuan Q, Zhang W, et al. Low-emissivity interior wall strategy for suppressing overcooling in radiatively cooled buildings in cold environments. Sustain Cities Soc, 2023, 99: 104912
13 Zhang X, Li X, Wang F, et al. Low-cost and large-scale producible biomimetic radiative cooling glass with multiband radiative regulation performance. Adv Opt Mater, 2022, 10: 2202031
14 Zhao D, Aili A, Yin X, et al. Roof-integrated radiative air-cooling system to achieve cooler attic for building energy saving. Energy Buildings, 2019, 203: 109453
15 Zou H, Wang C, Yu J, et al. Eliminating greenhouse heat stress with transparent radiative cooling film. Cell Rep Phys Sci, 2023, 4: 101539
16 Ahmed S, Li S, Li Z, et al. Enhanced radiative cooling of solar cells by integration with heat pipe. Appl Energy, 2022, 308: 118363
17 Zhao B, Lu K, Hu M, et al. Radiative cooling of solar cells with micro-grating photonic cooler. Renew Energy, 2022, 191: 662–668
18 Bellos E, Tzivanidis C. A detailed investigation of an evacuated flat plate solar collector. Appl Thermal Eng, 2023, 234: 121334
19 Chen M, Pang D, Yan H. Highly solar reflectance and infrared transparent porous coating for non-contact heat dissipations. iScience, 2022, 25: 104726
20 Zhang X, Cheng Z, Yang D, et al. Scalable bio-skin-inspired radiative cooling metafabric for breaking trade-off between optical properties and application requirements. ACS Photonics, 2023, 10: 1624–1632
21 Gu B, Xu Q, Wang H, et al. A hierarchically nanofibrous self-cleaning textile for efficient personal thermal management in severe hot and cold environments. ACS Nano, 2023, 17: 18308–18317
22 Li J, Liang Y, Li W, et al. Protecting ice from melting under sunlight *via* radiative cooling. Sci Adv, 2022, 8: eabj9756
23 Jing W, Zhang S, Zhang W, et al. Scalable and flexible electrospun film for daytime subambient radiative cooling. ACS Appl Mater Interfaces, 2021, 13: 29558–29566
24 Pan H, Zhao D. An improved model for performance predicting and optimization of wearable thermoelectric generators with radiative cooling. Energy Convers Manage, 2023, 284: 116981
25 Dong Y, Wang F, Zhang Y, et al. Experimental and numerical study on flow characteristic and thermal performance of macro-capsules phase change material with biomimetic oval structure. Energy, 2022, 238: 121830
26 Wu Y J, Liu B, Zhang R Y, et al. Temperature-adaptive porous polymer radiative cooling coatings for all-season thermal management and annual energy-saving. Energy Buildings, 2023, 296: 113423
27 Dong Y, Meng W, Wang F, et al. "Warm in winter and cool in summer": Scalable biochameleon inspired temperature-adaptive coating with easy preparation and construction. Nano Lett, 2023, 23: 9034–9041
28 Liu J, Tang H, Jiang C, et al. Micro-nano porous structure for efficient daytime radiative sky cooling. Adv Funct Mater, 2022, 32: 2206962
29 Shi N N, Tsai C C, Camino F, et al. Keeping cool: Enhanced optical reflection and radiative heat dissipation in Saharan silver ants.

Science, 2015, 349: 298–301
30 Zhai Y, Ma Y, David S N, et al. Scalable-manufactured randomized glass-polymer hybrid metamaterial for daytime radiative cooling. Science, 2017, 355: 1062–1066
31 Mandal J, Fu Y, Overvig A C, et al. Hierarchically porous polymer coatings for highly efficient passive daytime radiative cooling. Science, 2018, 362: 315–319
32 Luo X G. Principles of electromagnetic waves in metasurfaces. Sci China-Phys Mech Astron, 2015, 58: 594201
33 Zeng C, Lu H, Mao D, et al. Graphene-empowered dynamic metasurfaces and metadevices. Opto-Electron Adv, 2022, 5: 200098
34 Pu M, Guo Y, Li X, et al. Revisitation of extraordinary Young's interference: From catenary optical fields to spin–orbit interaction in metasurfaces. ACS Photonics, 2018, 5: 3198–3204
35 Krasikov S, Tranter A, Bogdanov A, et al. Intelligent metaphotonics empowered by machine learning. Opto-Electron Adv, 2022, 5: 210147
36 Xu J, Wan R, Xu W, et al. Colored radiative cooling coatings using phosphor dyes. Mater Today Nano, 2022, 19: 100239
37 Wang X, Liu X, Li Z, et al. Scalable flexible hybrid membranes with photonic structures for daytime radiative cooling. Adv Funct Mater, 2020, 30: 1907562
38 Miao D, Cheng N, Wang X, et al. Integration of Janus wettability and heat conduction in hierarchically designed textiles for all-day personal radiative cooling. Nano Lett, 2022, 22: 680–687
39 Gentle A R, Smith G B. Radiative heat pumping from the earth using surface phonon resonant nanoparticles. Nano Lett, 2010, 10: 373–379
40 Li P, Wang A, Fan J, et al. Thermo-optically designed scalable photonic films with high thermal conductivity for subambient and above-ambient radiative cooling. Adv Funct Mater, 2022, 32: 2109542
41 Sun J, Wang J, Guo T, et al. Daytime passive radiative cooling materials based on disordered media: A review. Sol Energy Mater Sol Cells, 2022, 236: 111492
42 Cheng Z, Han H, Wang F, et al. Efficient radiative cooling coating with biomimetic human skin wrinkle structure. Nano Energy, 2021, 89: 106377
43 Long L, Yang Y, Wang L. Simultaneously enhanced solar absorption and radiative cooling with thin silica micro-grating coatings for silicon solar cells. Sol Energy Mater Sol Cells, 2019, 197: 19–24
44 Cheng Z, Wang F, Wang H, et al. Effect of embedded polydisperse glass microspheres on radiative cooling of a coating. Int J Thermal Sci, 2019, 140: 358–367
45 Wang C, Zhang Y, Hou H, et al. Entropy production diagnostic analysis of energy consumption for cavitation flow in a two-stage LNG cryogenic submerged pump. Int J Heat Mass Transfer, 2019, 129: 342–356
46 Wang S, Wu Y, Pu M, et al. A versatile strategy for concurrent passive daytime radiative cooling and sustainable energy harvesting. Small, 2024, 20: 2305706
47 Huang Z, Ruan X. Nanoparticle embedded double-layer coating for daytime radiative cooling. Int J Heat Mass Transfer, 2017, 104: 890–896
48 Bao H, Yan C, Wang B, et al. Double-layer nanoparticle-based coatings for efficient terrestrial radiative cooling. Sol Energy Mater Sol Cells, 2017, 168: 78–84
49 Dong Y, Zou Y, Li X, et al. Introducing masking layer for daytime radiative cooling coating to realize high optical performance, thin thickness, and excellent durability in long-term outdoor application. Appl Energy, 2023, 344: 121273
50 Dong Y, Han H, Wang F, et al. A low-cost sustainable coating: Improving passive daytime radiative cooling performance using the spectral band complementarity method. Renew Energy, 2022, 192: 606–616
51 Bu K, Huang X, Li X, et al. Consistent assessment of the cooling performance of radiative cooling materials. Adv Funct Mater, 2023, 33: 2307191